



# 26th International Symposium on Spin Physics

A Century of Spin



山东大学  
SHANDONG UNIVERSITY

# Polarized Energy-Energy Correlator in Jets at STAR

Ting Lin (林挺), for the STAR Collaboration  
Shandong University (山东大学)



Supported in part by

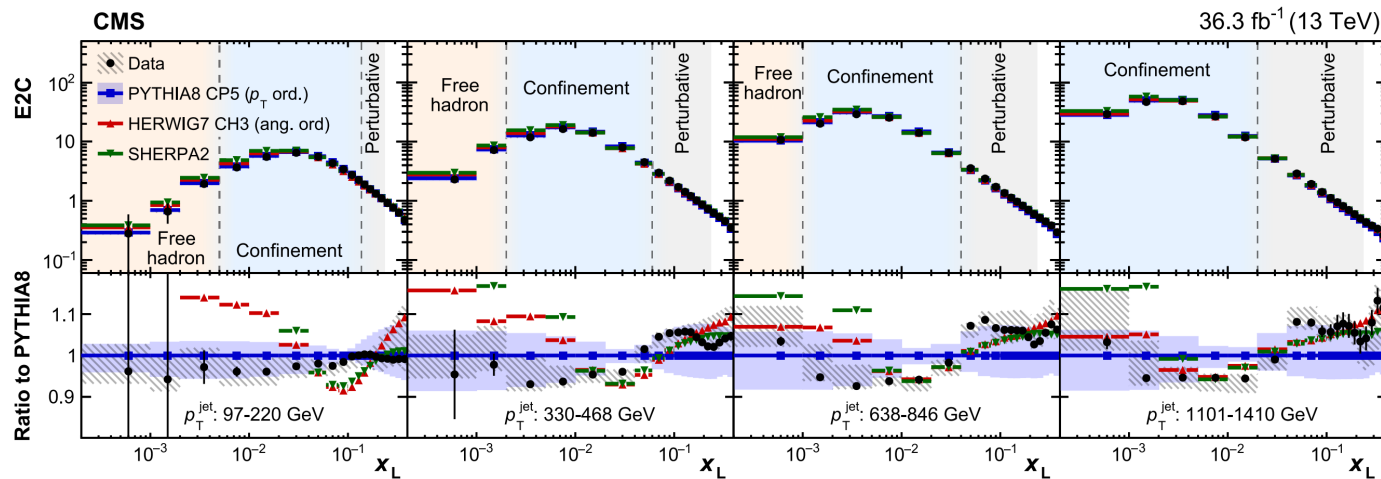


U.S. DEPARTMENT OF  
**ENERGY**

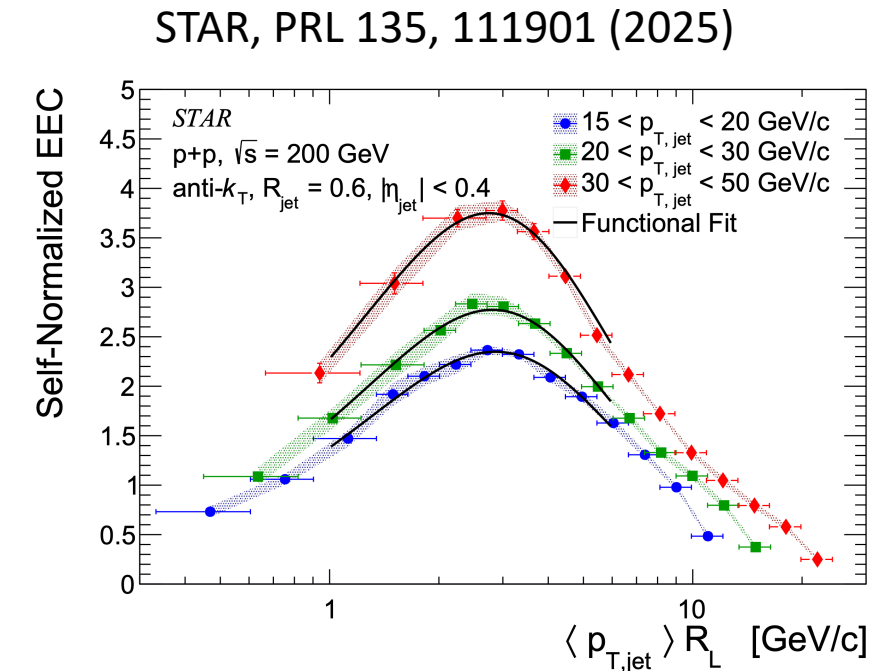
Office of  
Science

# EEC in Jets

- Originally introduced in  $e^+e^-$  annihilation, EECs have been extended to hadronic collisions and jet substructure studies;
- Measures the angular correlation of energy flow in jets, providing insight into the underlying QCD dynamics and parton structure.



CMS, PRL 133, 071903 (2024)

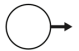



# Polarized EEC in Jets

Xiaohui Liu, Hua Xing Zhu, PRL 130.091901 (2023)

- Infrared and collinear safe; angular separation directly probes parton-to-hadron evolution;
- Project spin-dependent fragmentation functions onto Mellin moments, avoiding full TMD fits;
  - Access to higher order Mellin moment with weight of  $z_h^{N-1}$ , difficult in other observables;
- Provide new, controlled constraints on spin-momentum correlations in hadronization.

TMD Handbook, arXiv:2304.03302 [hep-ph]

Leading Quark TMDFFs  Hadron Spin  Quark Spin

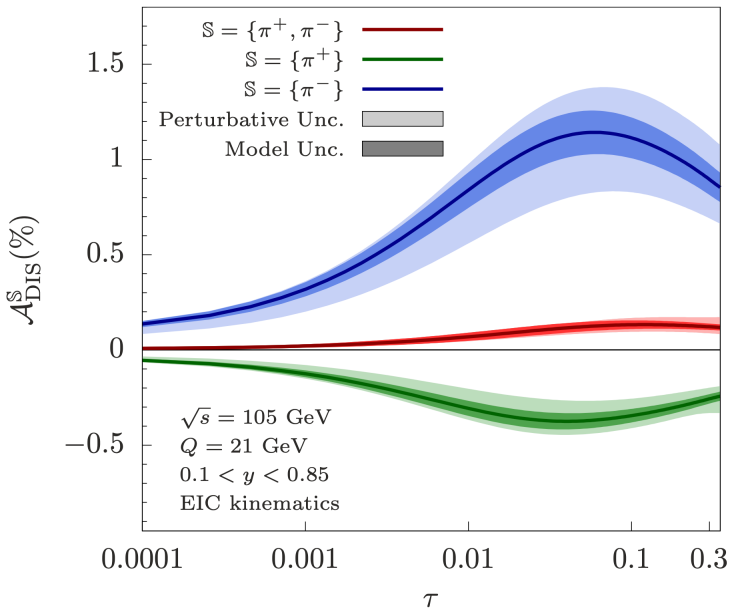
		Quark Polarization		
		Un-Polarized (U)	Longitudinally Polarized (L)	Transversely Polarized (T)
Unpolarized (or Spin 0) Hadrons		$D_1 = \text{Unpolarized}$		$H_1^\perp = \text{Collins}$
Polarized Hadrons	L		$G_1 = \text{Helicity}$	$H_{1L}^\perp$
	T	$D_{1T}^\perp = \text{Polarizing FF}$	$G_{1T}^\perp$	$H_1^\perp = \text{Transversity}$ $H_{1T}^\perp$

SPIN 2025

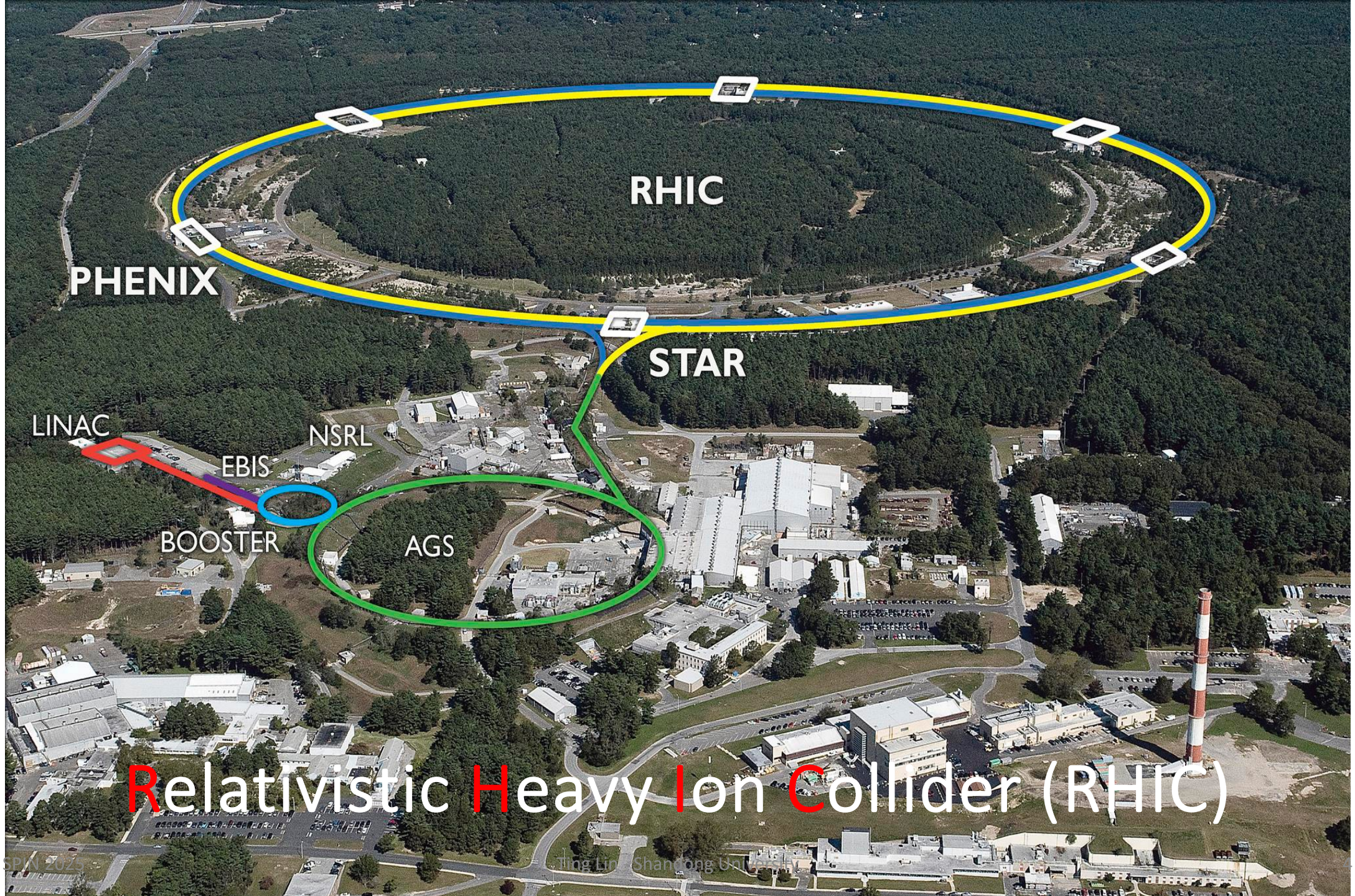
Zhong-Bo Kang, Kyle Lee, Ding Yu Shao & Fanyi Zhao JHEP 03 (2024) 153

$$\begin{aligned}
 & \frac{-\epsilon_T^{ab} n_i^a S_T^b}{M_P} f_{T,\text{EEC}}^q(N, \theta) \\
 &= \sum_X \sum_{i \in X} z_b^{N-1} \frac{\vec{n} \cdot p_i}{P} \frac{\vec{n}}{2} \frac{\vec{n}}{2} \alpha\beta \\
 & \times \langle P, S_T | \bar{\chi}_n \delta_{z_i P, P_n} \delta^{(2)}(\vec{n}_t - \vec{n}_{i,t}) | X \rangle_\alpha \langle X | \chi_n | P, S_T \rangle_\beta,
 \end{aligned}$$

Ting Lin - Shandong University







PHENIX

RHIC

STAR

LINAC

NSRL

EBIS

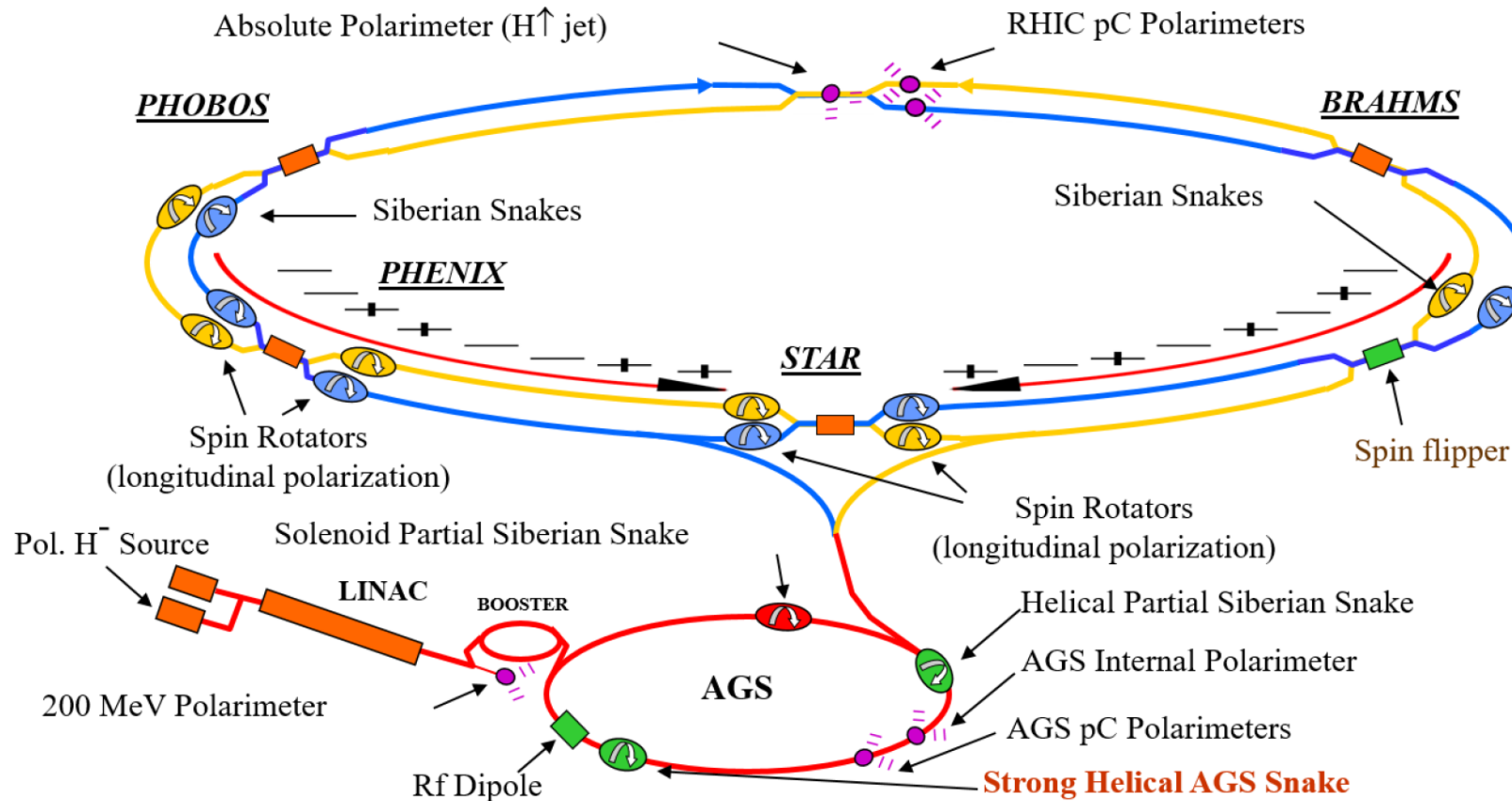
BOOSTER

AGS

Relativistic Heavy Ion Collider (RHIC)

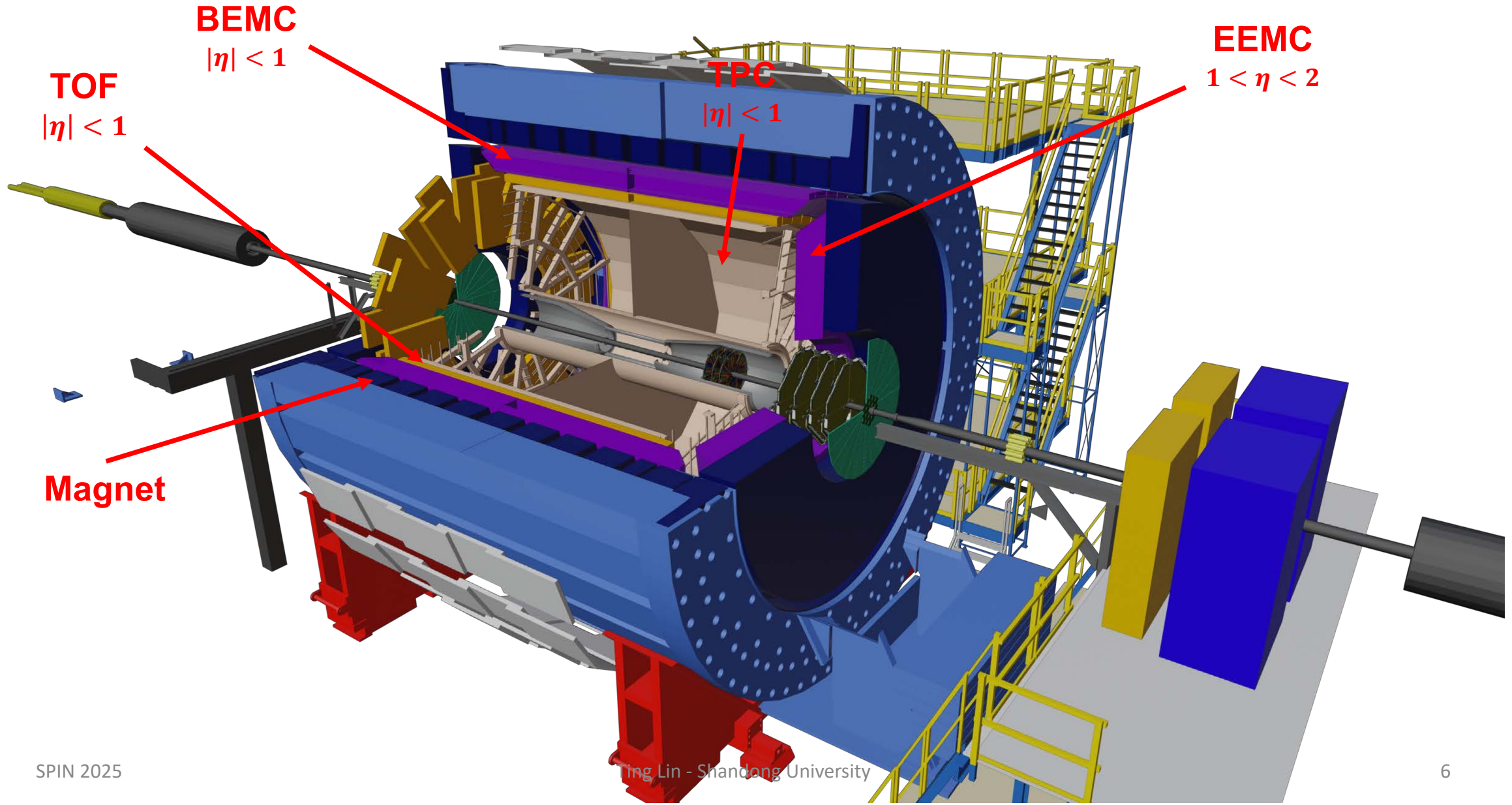


# Relativistic Heavy Ion Collider (RHIC)



- Spin pattern changes from fill to fill with little depolarization;
- Siberian snakes preserve the polarization;
- Spin rotators select spin orientation;
- proton-Carbon (pC) polarimeters and hydrogen gas jet (H-Jet) measure the polarization.

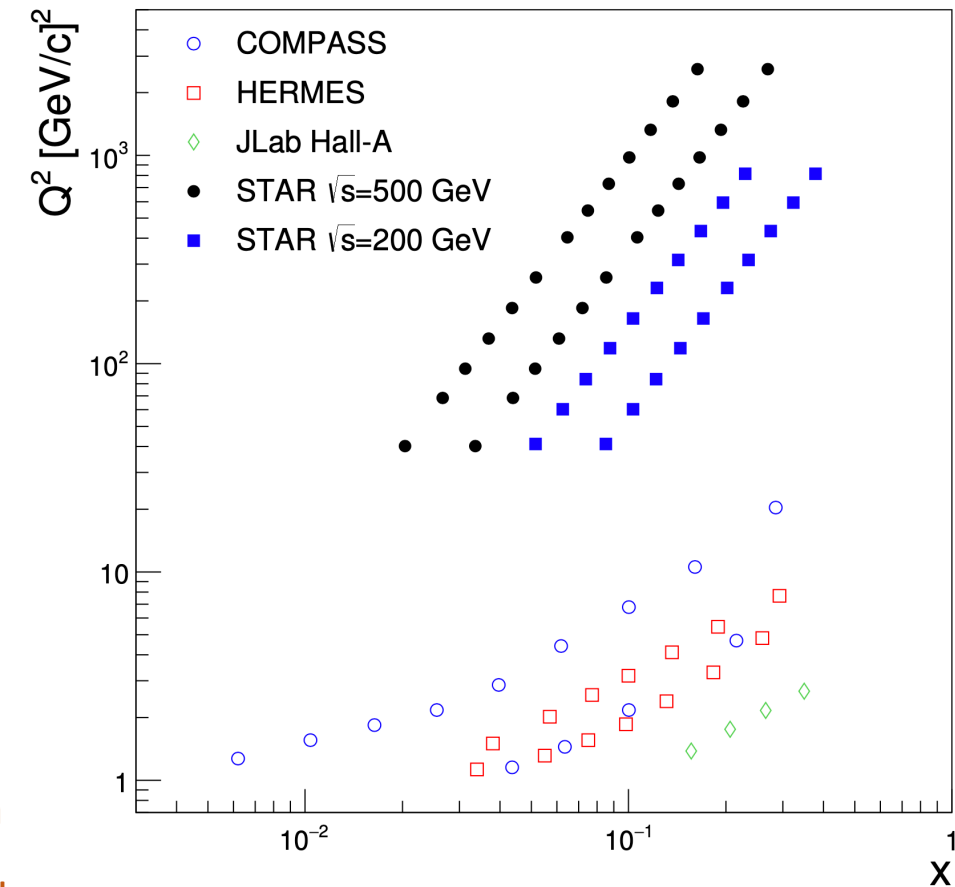
# Solenoidal Tracker At RHIC (STAR)



# STAR Data and Kinematic Coverage

Year	2011	2012	2015			2017	2022	2024
$\sqrt{s}$ (GeV)	500	200	200	200	200	510	508	200
$L_{int}$ ( $pb^{-1}$ )	23	22	pp	pAu	pAl	320	432	164
			52	0.42	1			
Polarization	53%	57%	57%	60%	54%	55%	51%	55%

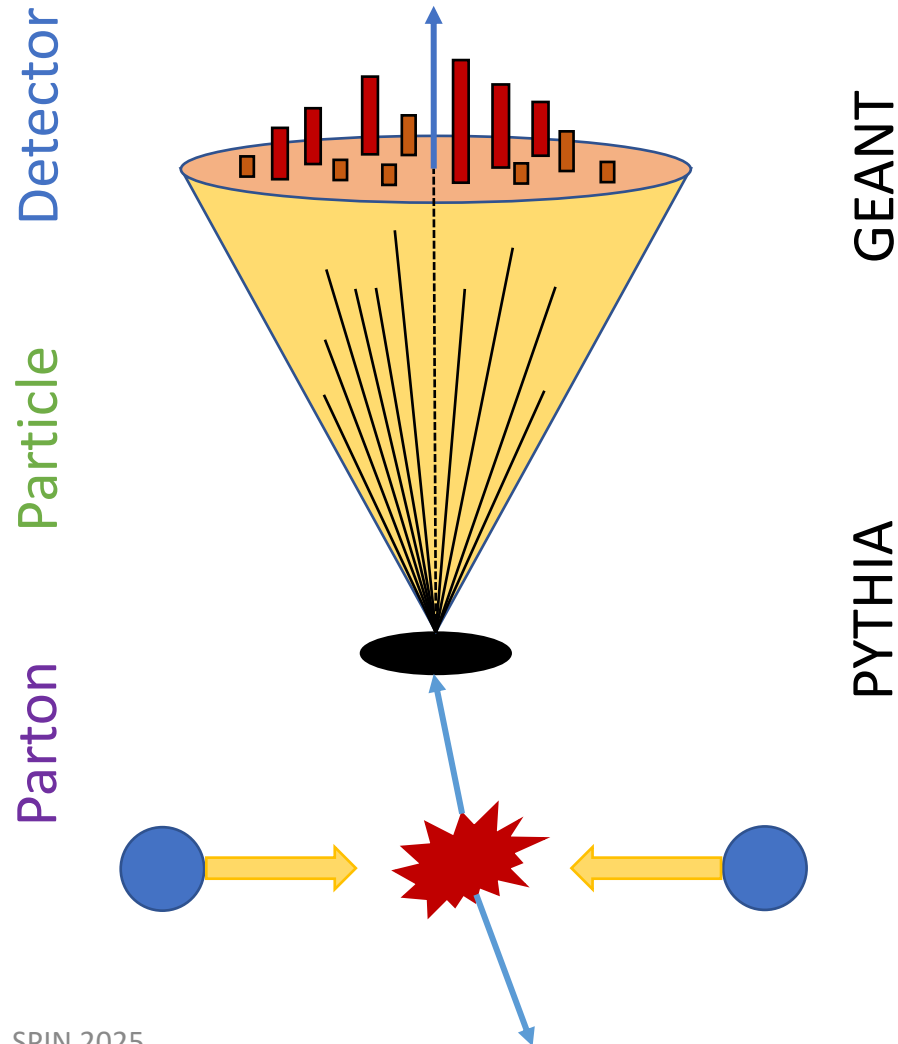
- STAR covers a similar range in momentum fraction to that of SIDIS experiments but at much higher  $Q^2$ ;
- 200 GeV results provide better statistical precision at larger momentum fraction regions while 500 GeV results probe lower values.
- These two different energies provide experimental constraints on evolution effects and insights into the magnitude and nature of TMD observables that will be measured at EIC.



# Jet Reconstruction

## Jet Levels

## MC Jets



## Anti- $K_T$ Algorithm:

- Radius = 0.6 for pp at  $\sqrt{s} = 200$  GeV, and 0.5 for pp at  $\sqrt{s} = 500$  GeV;
- Less sensitive to underlying event and pile-up effects;
- Used in both data and simulation;

## Simulation:

- PYTHIA 6.4 with STAR adjustment of Perugia 2012;

## Three Simulation Levels :

- Parton – hard scattered partons including ISR and FSR from Pythia;
- Particle – partons propagate and hadronize into stable and color-neutral particles;
- Detector – detector response to the stable particles.

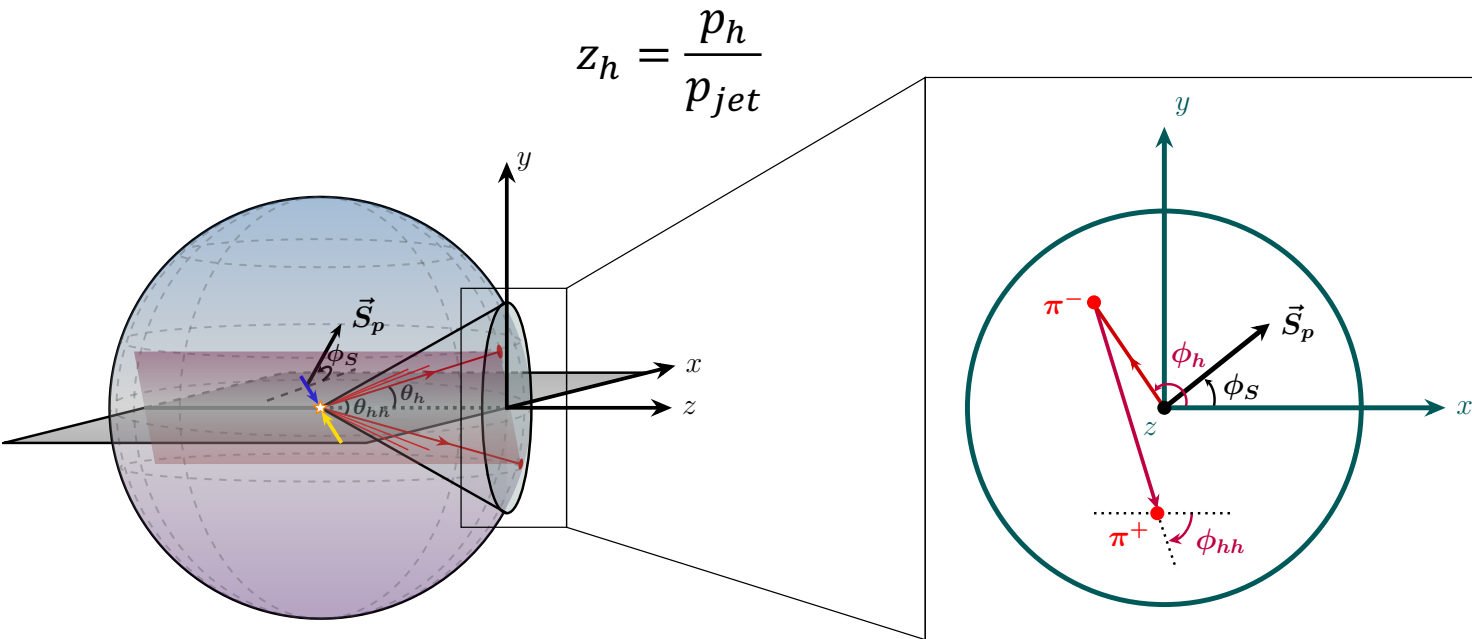


# EEC in $p^\uparrow p$ Collisions

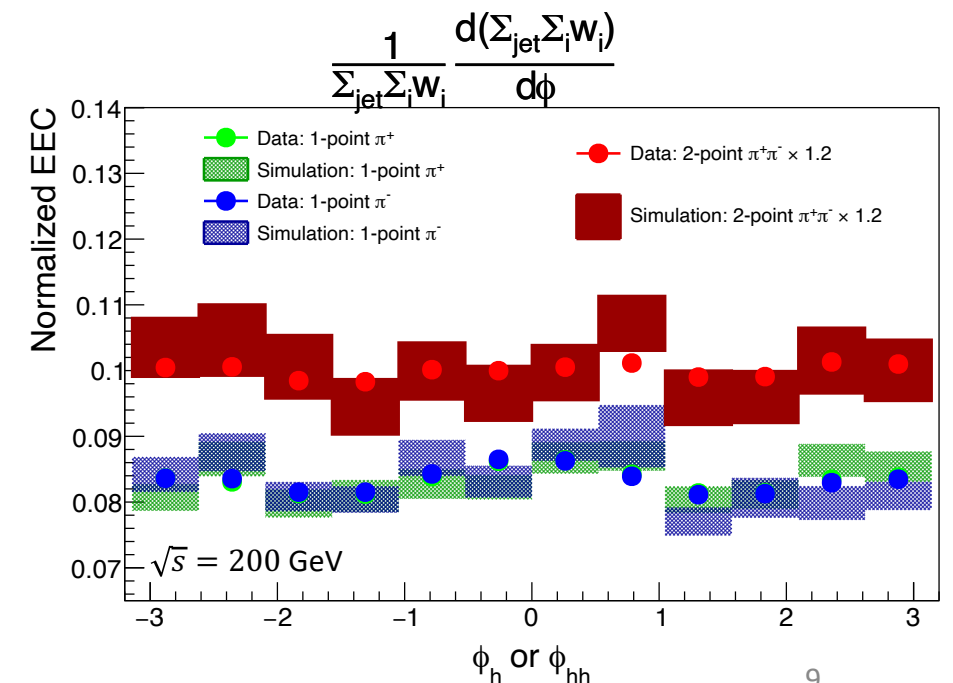
1-point,  $\theta_h$  is the angle between hadron and jet axis;

2-points,  $\theta_{hh}$  is the angle between two hadrons.

- For 1-point in jet,  $\text{EEC}(\theta_h, \phi_h) = \frac{d(\sum_{\text{jet}} \sum_i z_{h,i})}{d\theta_h d\phi_h}$ , loop over all hadrons in jet;
- For 2-point in jet,  $\text{EEC}(\theta_{hh}, \phi_{hh}) = \frac{d(\sum_{\text{jet}} \sum_{ij} z_{h,i} z_{h,j})}{d\theta_{hh} d\phi_{hh}}$ , loop over all pairs in jet.

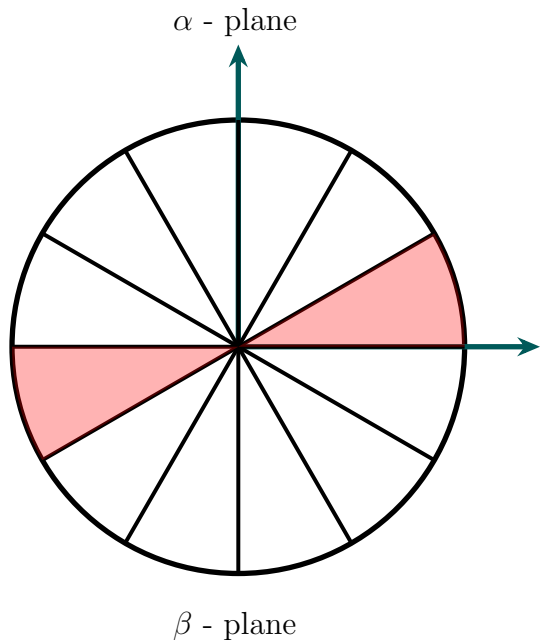


$$z_h = \frac{p_h}{p_{\text{jet}}}$$

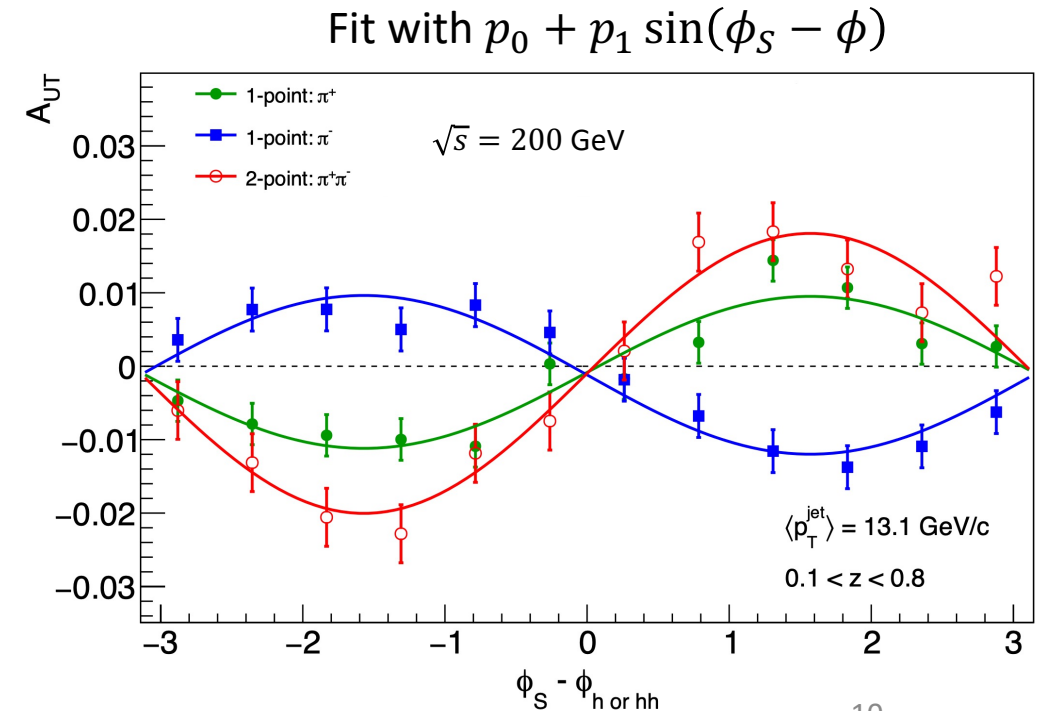


# Asymmetries vs. $\phi_S - \phi_{h/hh}$

$$A_{UT} = \frac{EEC^{\uparrow}(\phi_S - \phi) - EEC^{\downarrow}(\phi_S - \phi)}{EEC^{\uparrow}(\phi_S - \phi) + EEC^{\downarrow}(\phi_S - \phi)} = \frac{1}{P} \frac{\sqrt{EEC_{\alpha}^{\uparrow} EEC_{\beta}^{\downarrow}} - \sqrt{EEC_{\alpha}^{\downarrow} EEC_{\beta}^{\uparrow}}}{\sqrt{EEC_{\alpha}^{\uparrow} EEC_{\beta}^{\downarrow}} + \sqrt{EEC_{\alpha}^{\downarrow} EEC_{\beta}^{\uparrow}}}$$

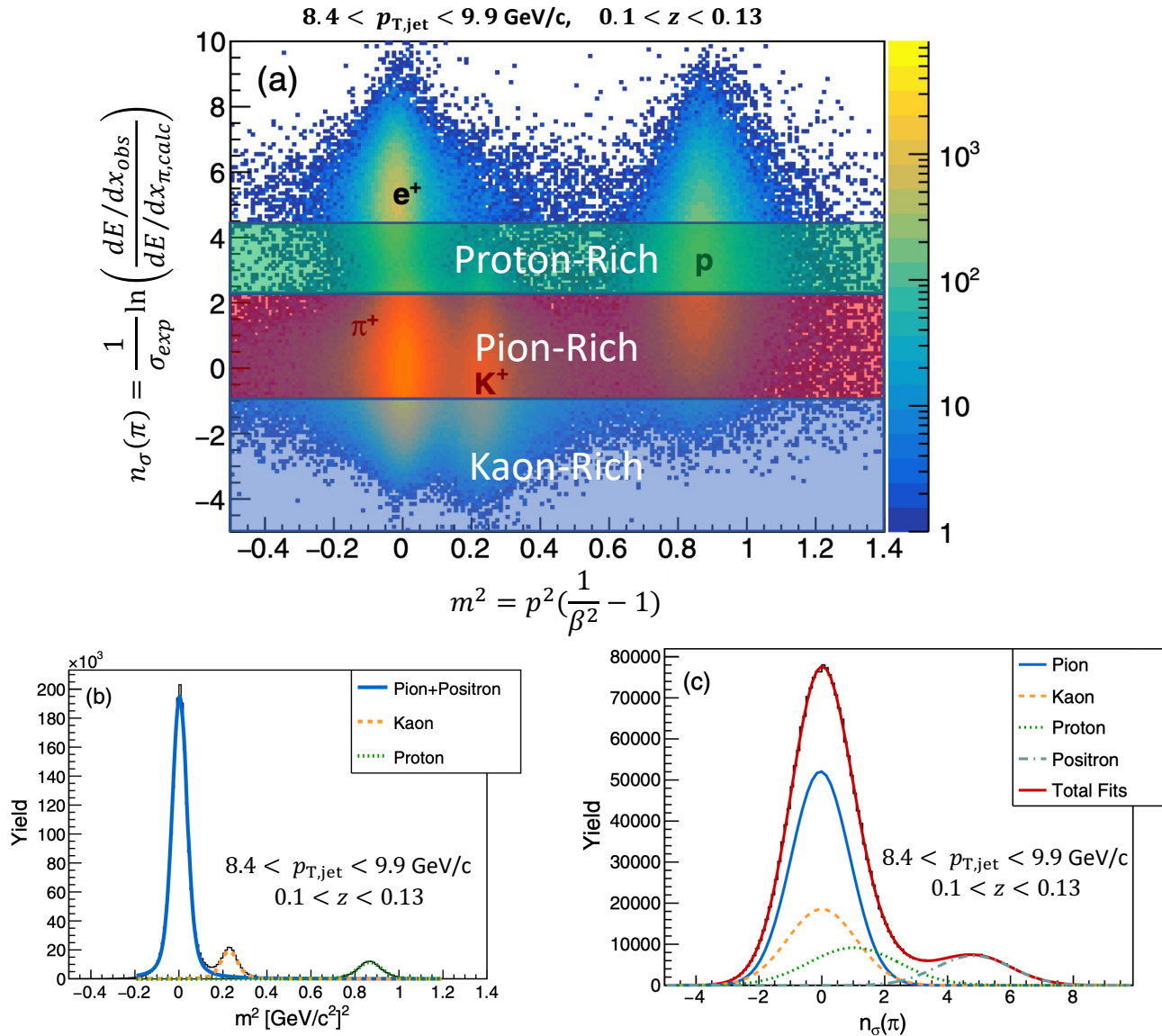


- Cross-ratio is used for asymmetry calculation;
- Detector separated into azimuthally opposite  $\alpha$  and  $\beta$  halves based on  $\phi_{jet}$ ;
  - Cancel out acceptance and luminosity effects;
  - Symmetry for  $EEC_{\alpha}^{\uparrow}$  and  $EEC_{\beta}^{\downarrow}$ ;
  - $\phi_S$  has the range of  $[-\frac{\pi}{2}, \frac{\pi}{2}]$ ;
  - $\phi_{h/hh}$  and  $\phi_S - \phi_{h/hh}$  have the range of  $[-\pi, \pi]$ ;





# Particle Identification Corrections



$$A_{raw} = (A_{\pi_{rich}}, A_{K_{rich}}, A_{p_{rich}})$$

$$A_{pure} = (A_{\pi}, A_K, A_p)$$

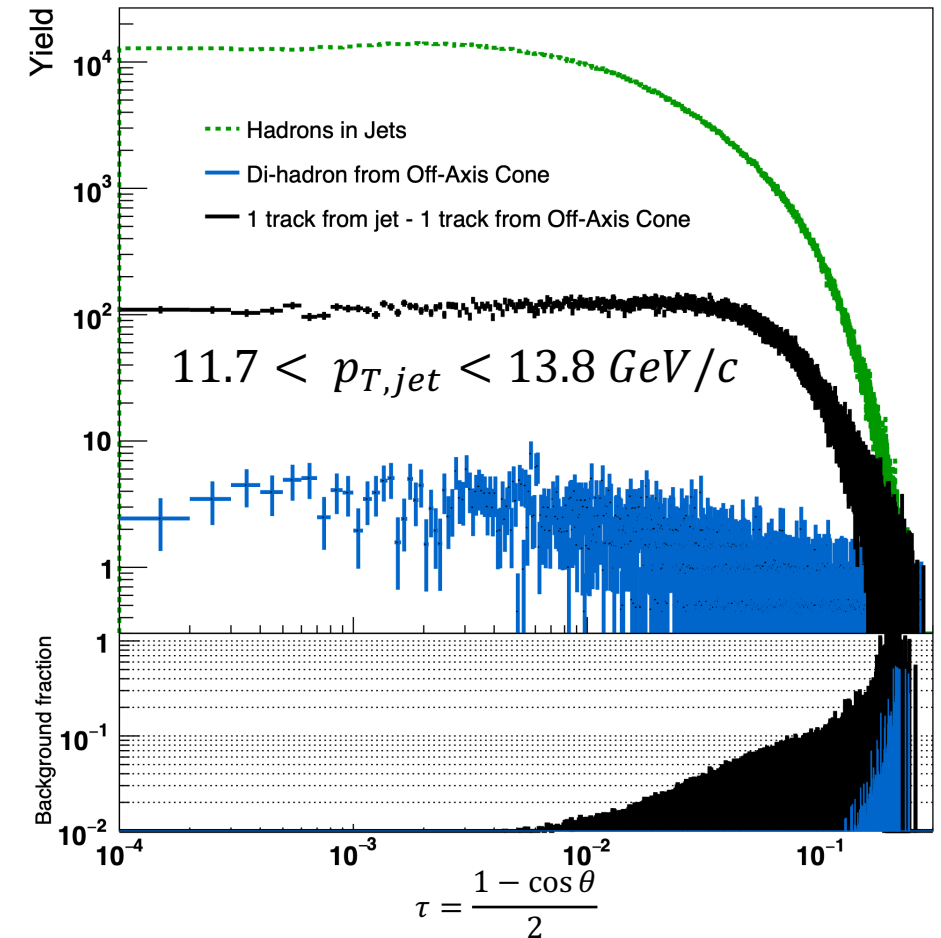
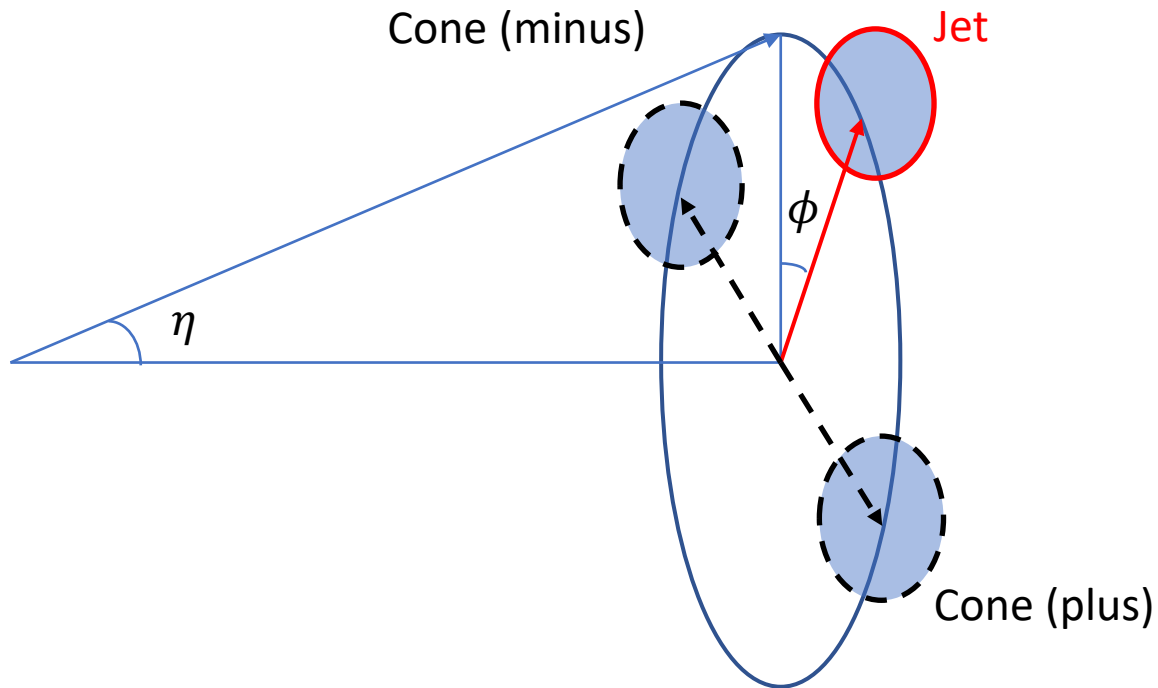
$$M = \begin{bmatrix} f_{\pi_{rich}}^{\pi} & f_{K_{rich}}^{\pi} & f_{p_{rich}}^{\pi} \\ f_{\pi_{rich}}^K & f_{K_{rich}}^K & f_{p_{rich}}^K \\ f_{\pi_{rich}}^p & f_{K_{rich}}^p & f_{p_{rich}}^p \end{bmatrix}$$

$$\text{We have } A_{raw} = A_{pure} M$$

$$\text{Then } A_{pure} = A_{raw} M^{-1}$$

# Underlying Event Correction

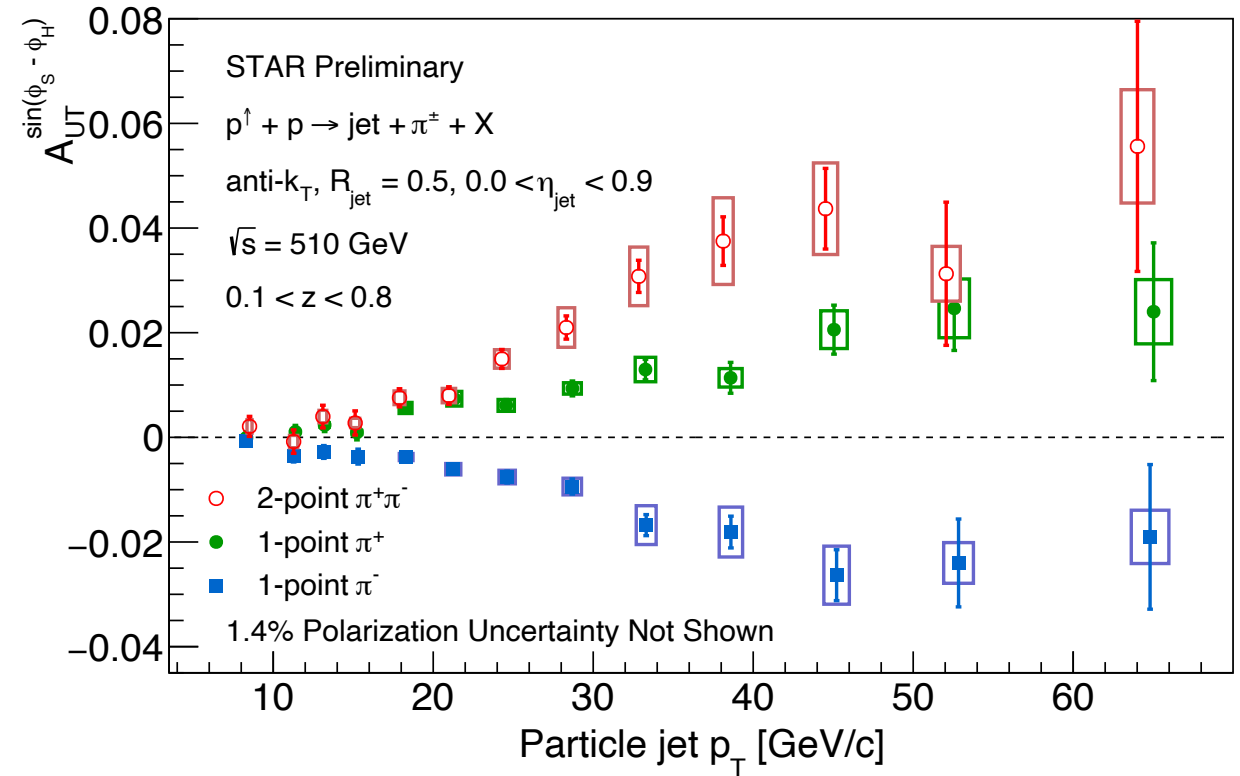
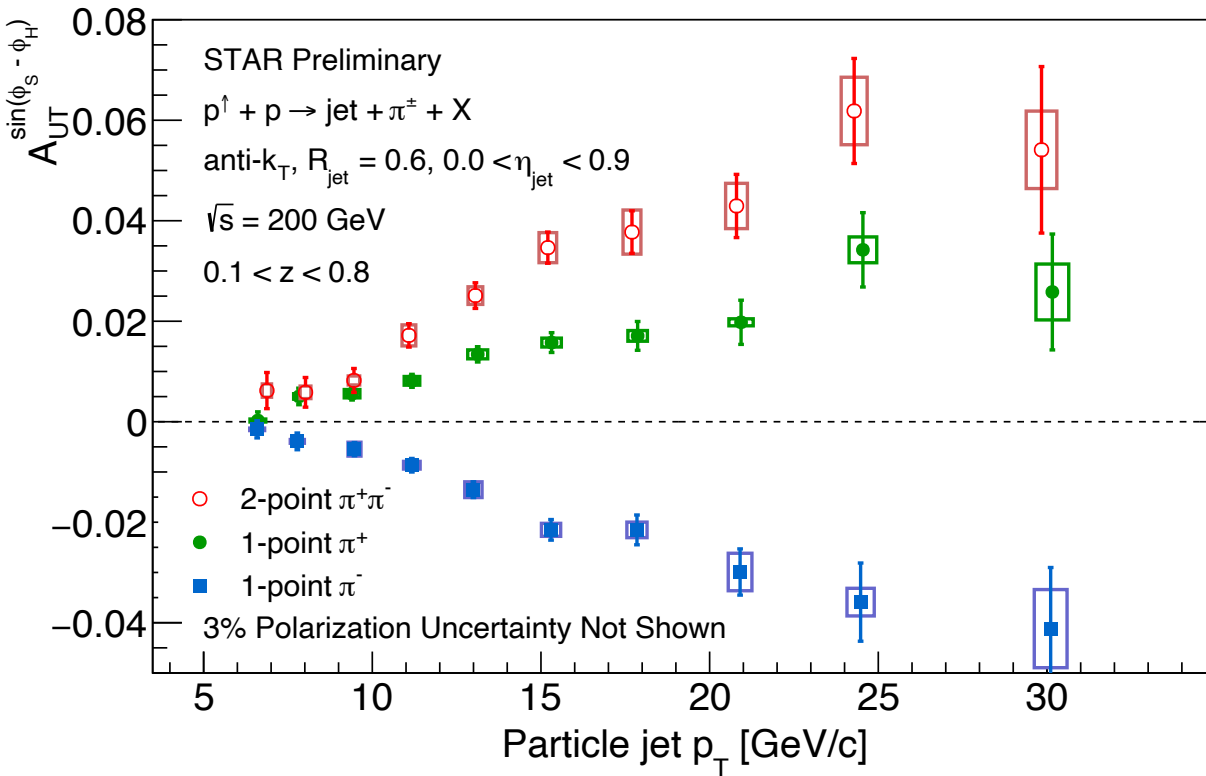
STAR, Phys. Rev. D **100**, 052005 (2019)



- Jet  $p_T$  values are corrected for underlying event activity measured using the off-axis cone method;
- Underlying event contribution to the spin asymmetries is treated as dilution.

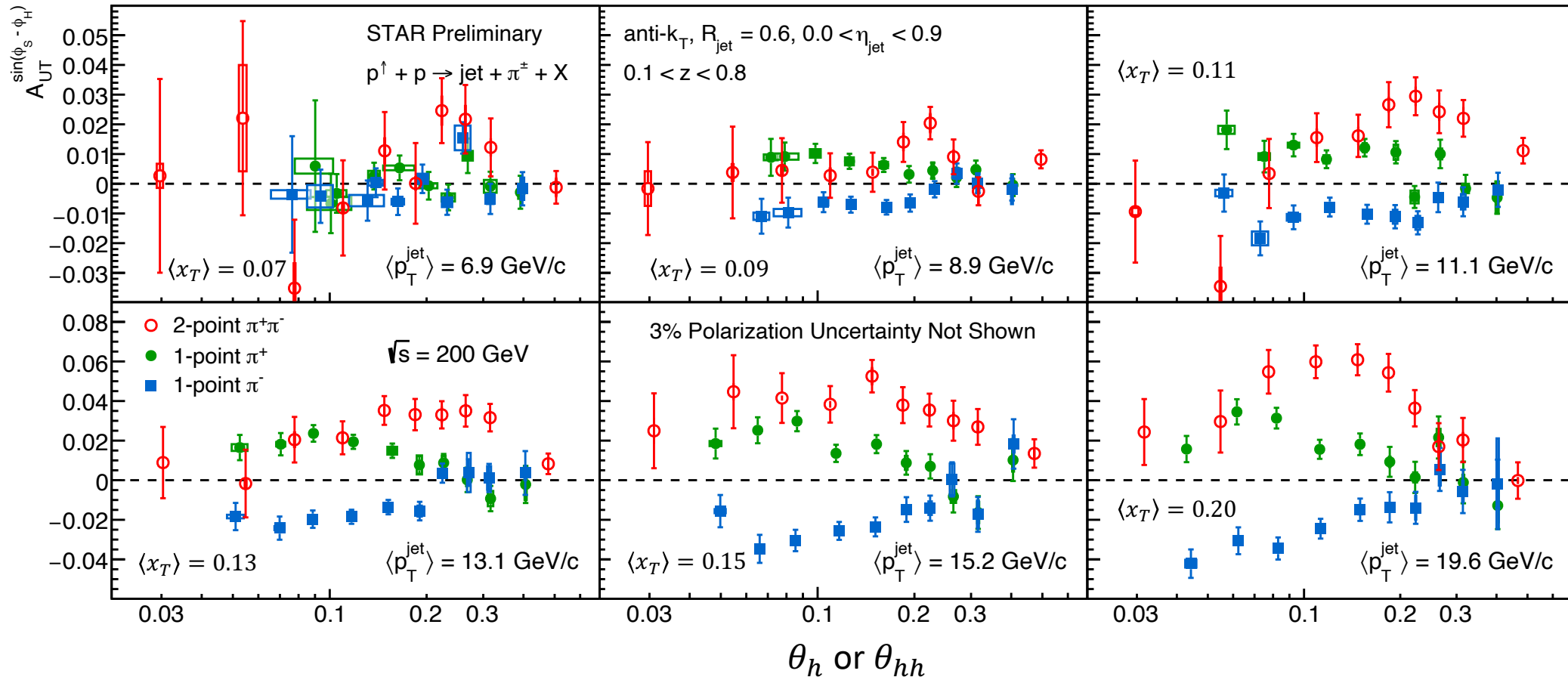


# EEC Asymmetries vs. $p_{T,jet}$



- Asymmetries increase vs. jet  $p_T$ , and can be as large as about 6% at this kinematic region;
- Two-point asymmetries align with one-point  $\pi^+$  results at low jet  $p_T$ , and are about twice at high jet  $p_T$ .

# EEC Asymmetries vs. $\theta_h$ or $\theta_{hh}$ , $\sqrt{s} = 200$ GeV

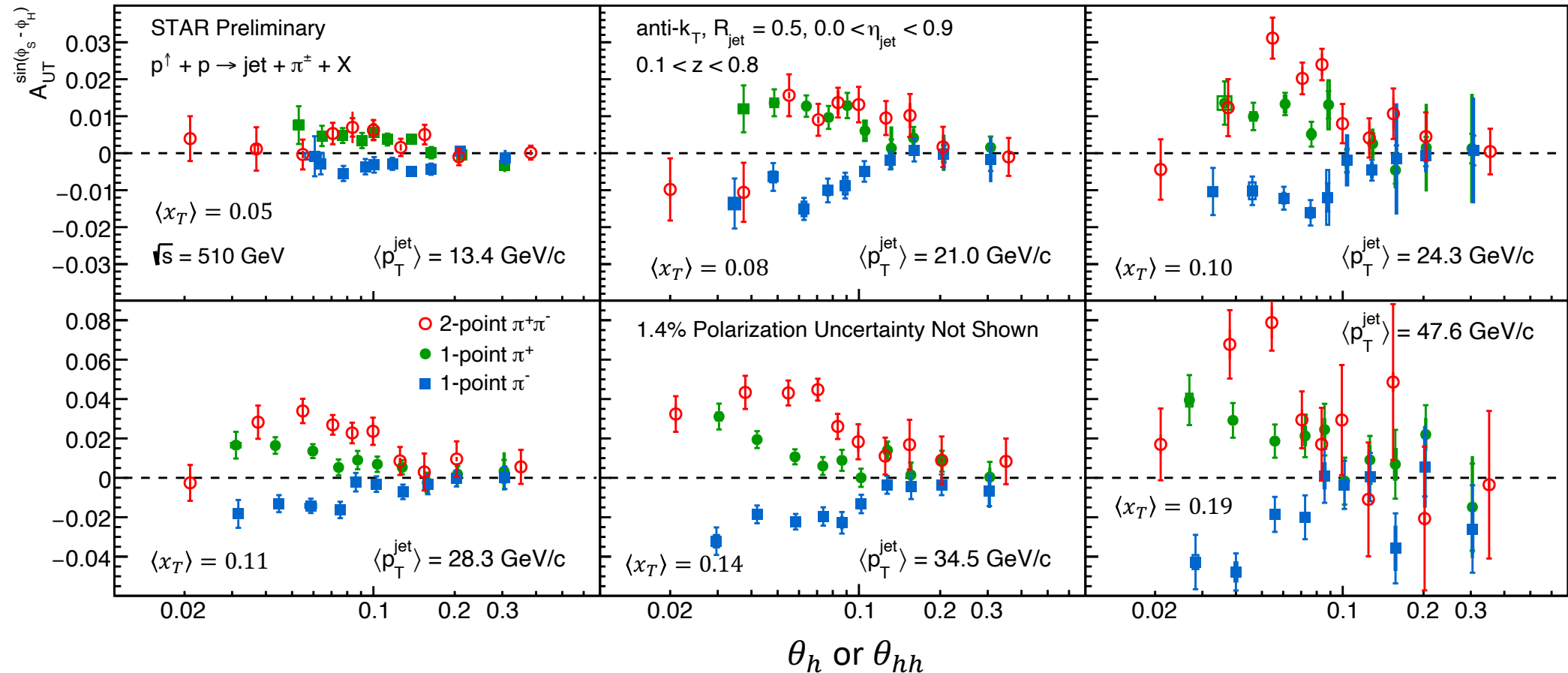


- Asymmetries change in different  $\theta$  values;
- The shape varies in different jet  $p_T$  bins.

1-point,  $\theta_h$  is the angle between hadron and jet axis;  
 2-points,  $\theta_{hh}$  is the angle between two hadrons.



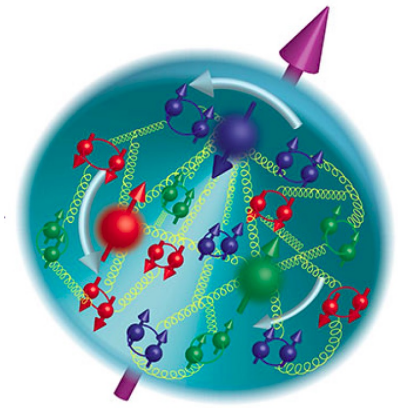
# EEC Asymmetries vs. $\theta_h$ or $\theta_{hh}$ , $\sqrt{s} = 510$ GeV



- Similar asymmetries observed at same  $x_T = 2p_{T,\text{jet}}/\sqrt{s}$  values;
- The shape varies in different jet  $p_T$  bins.

1-point,  $\theta_h$  is the angle between hadron and jet axis;  
 2-points,  $\theta_{hh}$  is the angle between two hadrons.

# Summary



- First measurement of one- and two-point EECs in transversely polarized pp collisions;
  - For one-point asymmetries,  $\pi^+$  has different sign as  $\pi^-$ ;
  - Asymmetries can be as large as about 6% for two-point results;
- A clear shape dependence vs. azimuthal separation is observed;
  - Varies in different jet  $p_T$  bins;
  - Theoretical interpretation would be helpful;
- Establishes EECs as new observables for transverse spin physics.